THERMAL STRESS CYCLING OF GaAs SOLAR CELLS

Robert W. Francis
The Aerospace Corporation
Los Angeles, California

Introduction

Thermal stress cycling has been performed on gallium arsenide (GaAs) solar cells to investigate their electrical, mechanical and structural integrity. Sponsored by the Defense Meteorological Satellite Program, cells were cycled under low earth orbit (LEO) simulated temperature conditions in vacuum. Over 15,000 thermal cycles from -80°C to +80°C have been imposed which equates to a three year mission in LEO. The test matrix consisted of thirty single junction GaAs solar cells (ten each from Applied Solar Energy Corporation (ASEC), Hughes Research Laboratories (HRL), and Varian Associates) which were characterized before, during and after the thermal cycling to establish performance parameters and trends. Cell evaluations consisted of measured AMO power output values, i.e., short-circuit current, open circuit voltage, fill factor, and efficiency, as well as spectral response, optical microscopy, and ion microprobe mass analysis (IMMA) depth profiles on both front surface inter-grid areas and metallization contact grid lines.

Cells were examined for performance degradation after 500; 5,000; 10,000 and a total 15,245 thermal cycles. Within the limitations of the experimental analysis, no indication of performance degradation was observed for any vendor's cell lot. The results presented here establish that, after 15,000 thermal stress cycles, the equivalent of three years in LEO, the cells have retained their power performance output with no loss of structural integrity or physical change in appearance.

Solar Cell Characteristics

All thirty (30) solar cells received for the thermal cycling experiment were single junction GaAs with a minimum of 16% (AMO) solar conversion efficiency reported by each vendor. Cells were 2 X 2 cm in area with a nominal 12 mil thickness, were fabricated in a P on N configuration and were supplied unglassed. Evaluation and analyses were carried out at various periods throughout the duration of the thermal stress cycling. Power output I/V measurements, spectral response, and optical microscopy were performed initially and after the 500; 5,000; 10,000 and 15,245 thermal cycles; whereas, cells were subjected to IMMA only initially and after thermal cycling was complete to minimize damage potentially incurred by the ion probe. Details of the preliminary results after 5,000 cycles utilizing these same analytical techniques have been published by B.K. Janousek et al, (Reference 1). A review of the beginning of life solar cell characteristics is presented below for completeness.

Each cell's current vs. voltage and spectral response signature were measured at the Jet Propulsion Laboratory (JPL). A 1-sun illumination AMO spectral content was established by a Spectrolab X-25 solar simulator. The cell temperature was maintained at 28°C. Beginning-of-life (BOL) efficiencies confirmed values measured at each vendor. These efficiencies were 16% and above and are listed in Table 1 along with the other pertinent parameters. Cells are listed in descending efficiency value with no correlation to vendor. The average efficiency for the total thirty cell lot at BOL was 16.66% with a 0.53% standard deviation.

External quantum efficiency or spectral response measurements were also performed at the Jet Propulsion Laboratory on two solar cells from each of the three vendors. Spectral response signatures exhibit the quantum efficiency as a function of photon energy and permit the cell's electrical performance to be probed as a function of the device's optical absorption characteristic in a specific layer. Thus, the spectral response signatures enable evaluation of potential factors that contribute to performance losses by determining which interior region of the

cell has degraed. BOL spectral response signatures all exhibit a sharp rise at approximately 900 nm to a maximum response of about 0.55 mA/mW followed by a gradual down slope in response at shorter wavelengths and then finally a sharp drop in response at less than 450 nm.

Due to potential device damage created by oxygen-18 ion drilling during the IMMA concentration depth profile analysis, only one sample from each of the three vendors was investigated. To minimize electrical damage to the cell the probed area was only 100 X 20 μm and located at the lower end of a grid line opposite the bus bar. Since front contact metal migration and diffusion into the junction region could be enhanced by temperature differential stress cycling, this needed to be considered as a possible degradation mechanism in GaAs causing cell shunting. IMMA metallization depth profiles were obtained on the p-contact side both on and between the grid lines. Concentration depth profiles were obtained before cycling, after 5,000 cycles and at cycling termination. Comparison of the signature curves gives a good indication of only enhanced metal diffusion or interfacial structural changes due to the imposed thermal stresses.

Finally, optical photomicrographs were taken on all 30 cells before and after completion of each cycle period. These photographs served as a historical record to compare the cell surface morphology, topography and potential grid line delamination caused by the thermal cycling stresses.

Thermal Stress Cycling

Temperature cycling is being conducted in The Aerospace Corporation's Aerophysics Laboratory. A picture of the apparatus is shown in Figure 1. The temperature oscillates from -80°C to +80°C with a sinusoidal temperature vs. time profile. No temperature dwell time is imposed at the temperature extremes. One cycle period is 0.5 Hr. and the operation is continuous and automatic. The cells thermal cycle in vacuum at a pressure less than 10^{-6} torr. Several safety features are

built into the microprocessor control unit. If the temperature approaches +100°C or -100°C, a fail-safe feature prohibits operation beyond these temperature extremes; if the vacuum system fails, cell cycling is discontinued and the chamber is returned to ambient temperature. A call-in feature allows equipment status checking during off hours. Monitoring and control thermistors are mounted at nine locations both inside and outside the temperature control block (Figure 2).

During temperature cycling, the solar cells occupy individual square slots in a covered aluminum picture frame configuration that is mounted to the temperature control block. There are a total of 36-1.0 in^2 slots for cells. Three 2 X 2 cm silicon solar cells provided by ASEC are also included in the thermal cycling test to provide a standard and enable an internal comparison for the GaAs thermal stress evaluation. The remaining three slots were occupied with electrically inactive mechanical GaAs cell blanks with thermistors attached with thermal conductive epoxy. This permitted active cell temperature monitoring by similarity. Three additional backup beaded thermocouples were mounted to the top of the cover plate by washers on the temperature control block and the final three thermocouples were also washer mounted on the cover plate top to provide temperature control and uniform temperature monitoring.

The thermal data obtained during the total 15,245 cycles is described in Table 2. T6 and T8 are thermocouples mounted on the cover plate at each end and T7 is mounted in the middle section. Thermistors attached to the GaAs mechanical blanks (T0, T1 and T2) were not utilized for temperature monitoring due to difficulty with maintaining an adherent thermistor contact to the GaAs surface during the temperature cycling. As a result, this resulted in anomalous temperature readings from these sensors.

Performance Results After 15,245 Thermal Cycles

Cell efficiency data after 500, 5,000, 10,000 and 15,245 cycles are listed in Table 3. In Table 4 are the performance parameters after 15,245 cycles for comparison of the BOL data in Table 1. Again, cells are listed in the same order as Table 1 with no correlation to vendor. One cell examined by IMMA demonstrated anomalous efficiency values when measured at each 5,000 cycle period, and the other two vendors' cells broke into 2-3 pieces each, possibly due to cracks initiated during IMMA analysis and propagating during temperature cycling. Thus, electrical performance data as a function of cycle number is not given for these three IMMA analyzed cells. In addition, three cells were unintentionally broken when the thermal vacuum chamber was last opened at 15,245 cycles. Fortunately, however, the three broken cells are spread evenly among each of the suppliers. A total of six cells, therefore, are not included in the final analysis. With a total of two cells each from three vendors excluded from the final cycle period data base the statistical comparison is maintained. This brings the total number to twenty-four cells which have successfully completed over 15,000 thermal cycles. These twenty-four solar cells have an average efficiency of 16.6% with a standard deviation of 0.6%. This is compared to an average efficiency of 16.7% with a 0.6% standard deviation for the same twenty-four cells (or a 16.7% and 0.5% standard deviation for all thirty cells) prior to thermal cycling. Within the experimental error of the efficiency measurement ($\pm 0.3\%$) no performance degradation is demonstrated after the total 15,245 LEO simulated thermal cycles. The average efficiency of the three reference silicon solar cells also compared closely within experimental error to the value of 13.4% before thermal cycling.

Both the external spectral response curves and IMMA depth profile signatures after 15,245 cycles indicated negligible change. The curves and signatures from pre and post cycling could, for the most part, be superimposed with no differences exhibited. Thermal stress cycling apparently has no effect on the optical absorption characteristics or

quantum efficiency of the devices nor has it any influence on enhancing the intermetallic contact diffusion, or changing the interlayer or interface structure. No indication of material redistribution was apparent as a result of thermal stress.

The optical micrographs taken after the 15,245 cycles demonstrated no change in the surface morphology or the topography of any cell. Furthermore, no grid line delamination was noticeable from temperature cycling.

Summary/Conclusions

Thermal stress cycling has been performed on GaAs solar cells under LEO simulated temperature conditions in vacuum. Over 15,000 cycles have been imposed which simulates a three year mission. The test matrix consisted of thirty GaAs solar cells (ten each from three suppliers) which were characterized and evaluated before, during and after completion of the thermal cycling. For reasons unrelated to the thermal stress cycling experiment, six cells were eliminated from the final cycle period data base. After a total 15,245 thermal cycles, the remaining twenty-four solar cells have an average efficiency of 16.6% compared to a 16.7% average efficiency prior to cycling. About three years of simulated thermal eclipses in LEO have been demonstrated with no performance degradation on ASEC, HRL, and Varian GaAs solar cells. This establishes the electrical, mechanical, and structural integrity during thermal stress cycling of single junction GaAs solar cells alone, i.e., without interconnects and coverglass.

No continued thermal cycling of the individual cells is presently being planned. At this time, the thermal cycling apparatus has been modified to accommodate panels fabricated by RCA Astro-Electronics and Spectrolab. These panels consist of both soldered and welded interconnected GaAs solar cell circuits. Preliminary thermal stress cycling results and analysis indicate stable performance.

References:

1. B.K. Janousek, R.W. Francis, and J.P. Wendt, "Thermal Stress Cycling of GaAs Solar Cells", Space Photovoltaic Research and Technology 1985, NASA CP-2408, April 1985, pp. 231-238.

TABLE 1

SOLAR CELL PRE-CYCLING ELECTRICAL PERFORMANCE PARAMETERS

Cell	Voc	Isc	FF	η
1.	1.015	116.8	0.814	17.82
2.	1.038	118.9	0.774	17.66
3.	1.031	119.4	0.776	17.65
4.	1.001	116.5	0.818	17.64
5.	1.017	112.7	0.814	17.24
6.	1.034	118.9	0.750	17.04
7.	1.030	117.8	0.759	17.03
8.	1.005	114.1	0.800	16.96
9.	1.018	119.8	0.750	16.90
10.	1.018	113.7	0.788	16.86
11.	0.993	114.3	0.804	16.86
12.	0.976	117.1	0.793	16.74
13.	1.013	111.3	0.803	16.73
14.	0.974	117.1	0.787	16.58
15.	1.033	117.1	0.740	16.55
16.	0.952	117.4	0.800	16.52
17.	1.018	118.0	0.743	16.50
18.	1.021	112.0	0.778	16.44
19.	0.950	115.2	0.808	16.34
20.	1.024	119.1	0.725	16.33
21.	0.987	111.6	0.802	16.32
22.	0.968	115.0	0.793	16.31
23.	1.005	110.6	0.793	16.29
24.	1.006	115.6	0.752	16.16
25.	1.009	113.0	0.766	16.14
26.	0.982	114.5	0.777	16.14
27.	1.006	111.2	0.780	16.11
28.	1.000	109.1	0.798	16.08
29.	0.989	113.7	0.773	16.07
30.	1.012	111.4	0.766	15.95
	1.004	115.1	0.781	16.66
	s=0.023	s=3.0	s=0.024	s=0.53

TABLE 2: TEMPERATURE VALUES FOR THE TOTAL 15,245 CYCLES

Minimum Temperatures (°C)

	T6	T7	T8
Average	-82.9	-81.1	-86.9
Standard Deviation	2.3	2.8	4.2
Minimum Minimum	-77.8	-62.3	-55.2
Maximum Minimum	-94.9	-91.9	-96.7

Maximum Temperatures (°C)

Average	84.8	86.9	85.9
Standard Deviation	2.8	2.7	3.4
Minimum Maximum	75.9	78.3	72.3
Maximum Maximum	90.7	93.1	93.8

TABLE 3

SOLAR CELL EFFICIENCY VS. CYCLING

Cell	η (0)	η (500)	η(5,000)	η(10,000)	η(15,245)
1.	17.82	17.62	17.45	17.53	17.71
2.	17.66	17.72	17.74	17.52	17.56
3.	17.65	17.56	17.64	17.51	17.65
4.	17.64	17.55	17.54	17.55	17.53
5.	17.24	17.05	17.00	17.00	-
6.	17.04	17.06	17.06	17.04	17.09
7.	17.03	16.95	17.00	16.82	16.94
8.	16.96	16.55	16.77	16.63	16.35
9.	16.90	(16.62)	-	-	-
10.	16.86	17.00	16.78	16.80	16.66
11.	16.86	16.86	16.90	16.80	16.88
12.	16.74	16.67	16.67	16.66	16.74
13.	16.73	16.54	16.69	16.81	16.67
14.	16.58	16.55	16.50	16.46	16.51
15.	16.55	16.64	16.53	16.43	16.66
16.	16.52	16.46	16.41	16.35	16.46
17.	16.50	16.52	16.40	15.80	15.95
18.	16.44	16.39	16.33	16.57	16.30
19.	16.34	(13.95)	-	-	-
20.	16.33	16.28	16.25	16.29	-
21.	16.32	16.32	16.20	16.31	16.26
22.	16.31	16.37	16.37	16.44	16.39
23.	16.29	(16.13)	-	-	-
24.	16.16	16.14	16.19	16.13	16.22
25.	16.14	16.18	16.05	16.00	15.68
26.	16.14	16.12	16.14	16.09	-
27.	16.11	15.94	16.00	15.88	15.82
28.	16.08	16.03	15.97	16.03	15.97
29.	16.07	16.18	16.09	16.05	16.04
30.	15.95	16.31	15.99	16.18	15.99
	16.66	16.65	16.62	16.58	16.58
	s=0.53	s=0.51	s=0.53	s=0.52	s=0.59

( ) ≡ AFTER IMMA

TABLE 4

SOLAR CELL PARAMETERS AFTER 15,245 CYCLES

Cell	Voc	Isc	FF	η
1.	1.012	118.3	0.801	17.71
2.	1.035	119.3	0.770	17.56
3.	1.029	119.0	0.780	17.65
4.	0.999	116.7	0.814	17.53
5.	-	-	-	-
6.	1.032	118.7	0.755	17.09
7.	1.027	118.0	0.757	16.94
8.	1.009	114.2	0.768	16.35
9.	-	-	-	-
10.	1.016	113.1	0.785	16.66
11.	0.991	115.3	0.799	16.88
12.	0.973	117.0	0.796	16.74
13.	1.011	111.3	0.802	16.67
14.	0.967	116.8	0.791	16.51
15.	1.031	117.5	0.744	16.66
16.	0.950	117.5	0.798	16.46
17.	1.013	118.5	0.719	15.95
18.	1.017	112.6	0.770	16.30
19.	-	-	-	-
20.	-	-	-	-
21.	0.985	111.5	0.802	16.26
22.	0.965	115.8	0.794	16.39
23.	-	-	-	-
24.	1.004	115.9	0.754	16.22
25.	1.006	112.2	0.752	15.68
26.	-	-	-	-
27.	1.002	110.7	0.772	15.82
28.	0.997	109.1	0.795	15.97
29.	0.986	113.0	0.780	16.04
20.	1.008	112.2	0.766	15.99
	1.003	115.2	0.778	16.58
	s=0.023	s=3.0	s=0.023	s=0.59

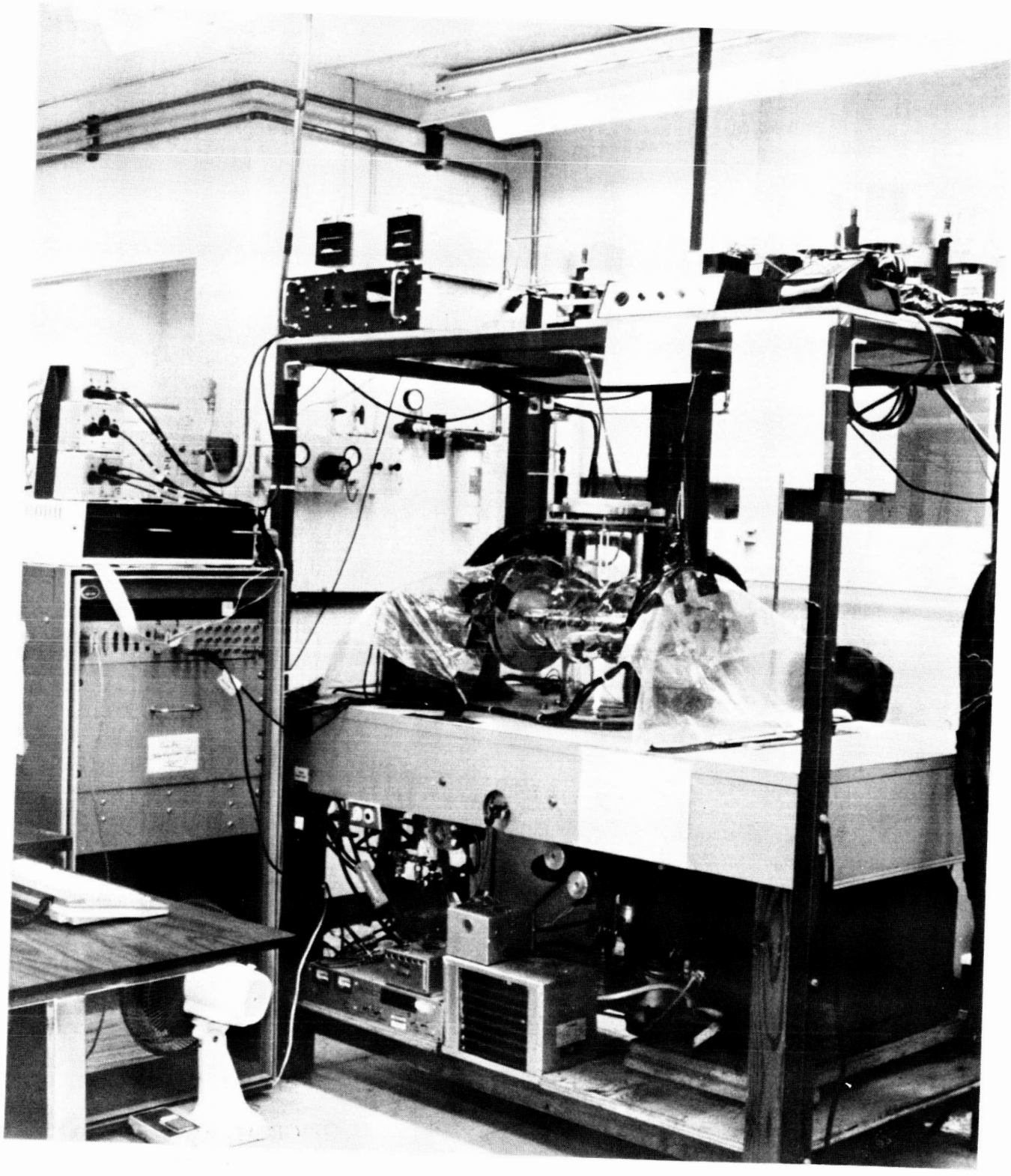

Figure 1

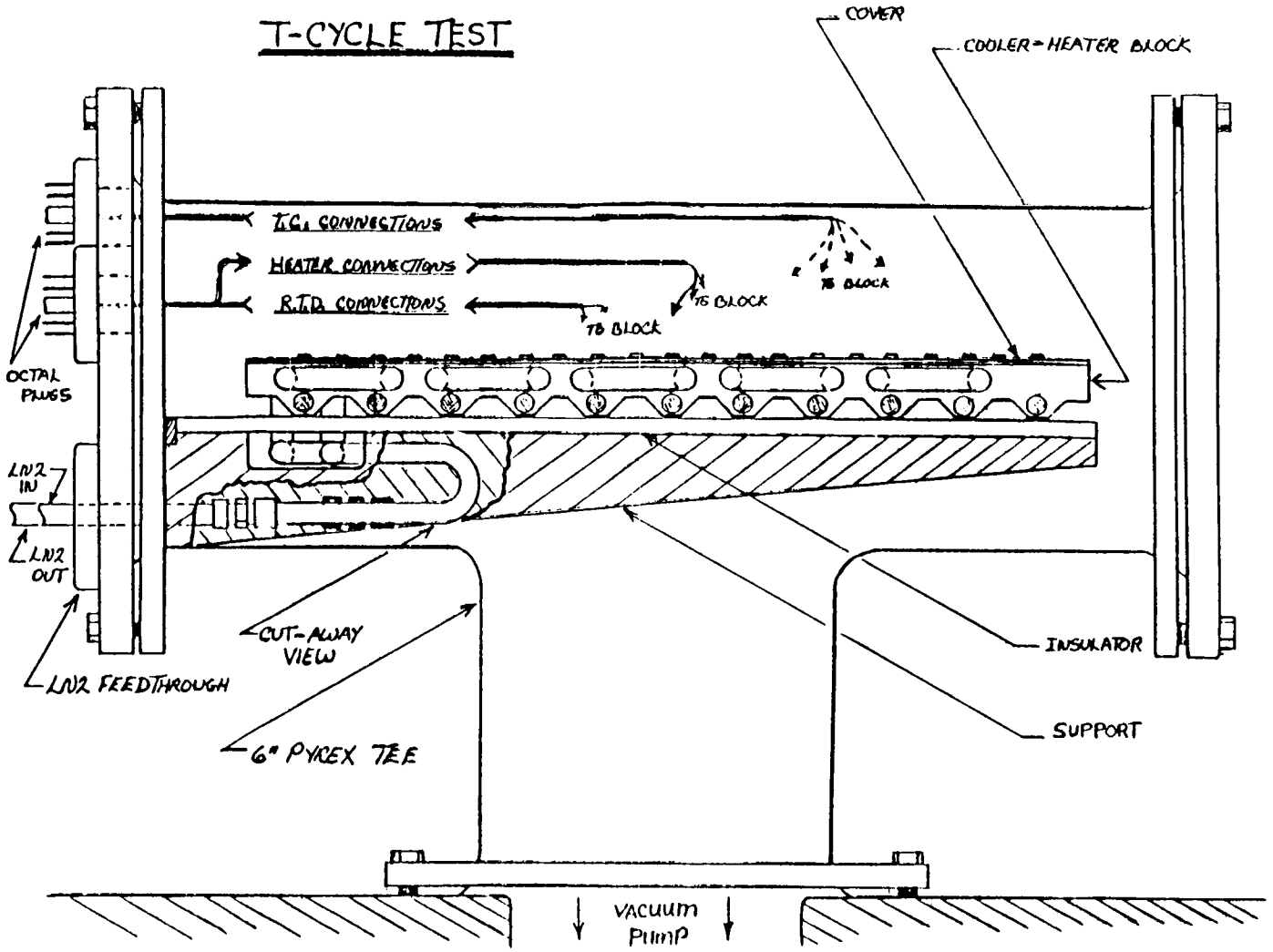

Figure 2

ORIGINAL PAGE IS
OF POOR QUALITY